



Since January 2020 Elsevier has created a COVID-19 resource centre with free information in English and Mandarin on the novel coronavirus COVID-19. The COVID-19 resource centre is hosted on Elsevier Connect, the company's public news and information website.

Elsevier hereby grants permission to make all its COVID-19-related research that is available on the COVID-19 resource centre - including this research content - immediately available in PubMed Central and other publicly funded repositories, such as the WHO COVID database with rights for unrestricted research re-use and analyses in any form or by any means with acknowledgement of the original source. These permissions are granted for free by Elsevier for as long as the COVID-19 resource centre remains active.

Identification of novel ligands for the RNA pseudoknot that regulate -1 ribosomal frameshifting

So-Jung Park,^{a,b} Young Hoon Jung,^a Yang-Gyun Kim^{b,*} and Hyun-Ju Park^{a,*}

^aCollege of Pharmacy, Sungkyunkwan University, Suwon 440-746, Republic of Korea

^bDepartment of Chemistry, Sungkyunkwan University, Suwon 440-746, Republic of Korea

Received 19 December 2007; revised 5 February 2008; accepted 8 February 2008

Available online 13 February 2008

Abstract—In many viruses, -1 ribosomal frameshifting (-1 RF) regulates synthesis of proteins and is crucial for virus production. An RNA pseudoknot is one of the essential components of the viral -1 RF system. Thermodynamic or kinetic control of pseudoknot folding may be important in regulating the efficiency of -1 RF. Thus, small molecules that interact with viral RNA pseudoknots may disrupt the -1 RF system and show antiviral activity. In this study, we conducted virtual screening of a chemical database targeting the X-ray crystal structure of RNA pseudoknot complexed with biotin to identify ligands that may regulate an -1 RF system containing biotin-aptamer as an RNA pseudoknot component. After docking screening of about 80,000 compounds, 58 high-ranked hits were selected and their activities were examined by *in vitro* and cell-based -1 frameshifting assays. Six compounds increased the efficiency of -1 frameshifting, and these are novel small molecule compounds that regulate the -1 RF.

© 2008 Elsevier Ltd. All rights reserved.

1. Introduction

In many viruses, programmed -1 ribosomal frameshifting (-1 RF) is a common recoding mechanism that regulates the relative expression of proteins that are encoded in two overlapping open reading frames (ORFs) during translation.¹ Programmed -1 RF has been shown in most retroviruses, corona viruses, yeast, and plant virus, and even in bacteria.^{2–8} The ORF encoding the major viral structural protein is located upstream of the -1 frameshift site, whereas ORFs encoding the enzymatic proteins are located downstream of -1 frameshift site. The major enzymatic proteins are only translated as a result of an -1 RF, which occurs with an efficiency of 1–30%, depending on the virus. This difference in efficiency suggests that the ratio of structural proteins to enzymatic proteins varies among viruses. If the efficiency of -1 RF in viruses is changed, it will dramatically change the ratio of related gene products and disrupt viral assembly.^{9,10} Since maintaining an accurate ratio is important for virus survival, altering the -1 RF efficiency interferes with the virus life cycle by eliminating or reducing viral production. There-

fore, -1 RF should be an excellent target for the development of antiviral agents. It has been already reported that the antibiotics, such as anisomycin, sparsomycin, and preussin, inhibit -1 RF and viral reproduction.¹¹

-1 RF requires three *cis*-acting elements in mRNA: slippery sequence, spacer, and pseudoknot. The slippery site consists of a heptamer sequence X XXY YYZ, where X can be any three identical nucleotides, Y is either A or U, and Z is A, U, or C; the spacer sequence separates codons in the initial (zero) frame. Mutagenesis studies showed that the spacer is necessary for efficient -1 RF. The ribosomal changes in reading frame occur in the slippery site during a ribosomal pause.^{12–14} The third element is usually a pseudoknot located five or six nucleotides (spacer) downstream from the slippery site. The pseudoknot induces the frameshifting by hindering the approaching ribosome and contributes to the probability of a reading-frame shift into the -1 frame.^{15–18} The function of the pseudoknot in the -1 RF was first identified using a signal derived from the avian corona virus infectious bronchitis, showing that the stability of the pseudoknot is critical for the efficiency of -1 RF.

The mechanism of -1 RF induced by the mRNA pseudoknot was explained by a mechanical model.^{19–22} When the elongating ribosome approaches the downstream pseudoknot in the zero frame, a stereochemical

Keywords: Structure-based virtual screening; -1 Ribosomal frameshifting; RNA pseudoknot; Biotin aptamer.

* Corresponding authors. Tel.: +82 31 299 4563; fax: +82 31 299 4575 (Y.G.K.); tel.: +82 31 290 7719; fax: +82 31 292 8800 (H.J.P.); e-mail addresses: ygkimmit@skku.edu; hyunju85@skku.edu

mismatch between the pseudoknot and helicase prevents helicase from unwinding the pseudoknot at the mRNA tunnel. The movement of the tRNA through the ribosome is resisted during translocation, because the wound pseudoknot is too large to enter the mRNA tunnel. As a result, the linker region between the A-site codon and the mRNA pseudoknot is stretched, causing tension in the linker mRNA. Because of this developed tension, mRNA strand moves one base in a (+) sense (3' direction). Therefore, the ribosome attempts to translocate the anticodon into the accurate P-site by the codon-anticodon reaction that places strain on the P-site tRNA, causing a bent conformation. As a result, the P-site tRNA codon-anticodon interaction is broken over the slippery site, causing relaxation of the tRNA in a (–) sense direction (5' direction). The tRNA can reassociate with the mRNA to generate the protein XXX YYY Z instead of X XXY YYZ in the –1 frame as the pseudoknot is denatured and elongation continues in the new reading frame.²²

RNA pseudoknots are formed when residues in a hairpin-loop base-pair with nucleotides outside the loop, yielding two stems that are connected by single-stranded loops.²³ One of the most common functions of the RNA pseudoknot is to induce –1RF, and the correctly folded viral RNA pseudoknot is an important feature for efficient –1RF. Thus, small molecules that interact with the pseudoknot with high affinity and selectivity would interfere with translational regulation and recoding in viruses. Therefore, the pseudoknot structures involved in –1RF are attractive targets for the development of antiviral therapies.²⁴

Although several three-dimensional structures of RNA pseudoknots involved in –1RF were solved,²⁵ only one structure of a RNA pseudoknot complexed with ligand has been reported. It is the high-resolution structure of the biotin-bound RNA aptamer (biotin-pseudoknot), in which biotin is bound at the interface between the stacked helices of the pseudoknot.²⁶

We are interested in identifying novel ligands for RNA pseudoknots involved in –1RF by structure-based virtual screening of a chemical database. In a successful case of RNA-targeted virtual screening, small molecule ligands for transactivation response (Tar) element of HIV virus were discovered by virtual screening and the ligands inhibit the Tar-TAT (transactivation protein) interaction, which is critical for HIV-1 replication in infected cells.^{27–29}

In this study, we first attempted to discover ligands that regulate the –1RF by interacting with RNA pseudoknot. We designed an –1RF system using a biotin-pseudoknot as an RNA component. The virtual screening of chemical database was conducted against the biotin-aptamer, and then select ligands were tested for their ability to affect the –1RF efficiency by *in vitro* and cell-based –1 frameshifting assays. We successfully identified ligands that altered –1 frameshifting efficiency. The current virtual screening strategy can be applied to discover agents against the RNA pseudoknot

in viruses that use the induced –1RF to synthesize proteins that are crucial for their propagation.

2. Results and discussion

2.1. Virtual screening of chemical database

The aim of this study was to discover ligands that alter the –1RF induced by a biotin-pseudoknot; thus we conducted a structure-based virtual screening of a chemical database. In the first step of the virtual screening, the program Unity³⁰ was used for preliminary filtering of the chemical database to select compounds that satisfied three-dimensional pharmacophore criteria based on the X-ray crystal structure of the biotin-pseudoknot (PDB id: 1F27). The RNA sequence used for this study is shown in Figure 1A. Biotin is bound at the interface between the stacked helices of the pseudoknot. The puckered thiophene ring is bound at the interface between the two helices and also forms hydrogen bonds with the last nucleotide in loop 2 (A26). The ureido ring is locked between the major groove edge of A26 and the U7 ribose and stabilized by forming a hydrogen bond with the exocyclic 2NH₂ of G6 (Fig. 1D).

The pharmacophore query for the Unity search consisted of a hydrogen bond acceptor atom and a hydrogen bond donor site, as shown in Figure 1D. The acceptor atom is the carbonyl oxygen atom of the ureido ring of biotin, which forms a hydrogen bond with G6, and the donor site is the ribose O4' atom of U7. About 80,000 compounds from chemical database³¹ were sent to a flexible Unity search. After the first filtering using Unity, 514 compounds were selected from the chemical database. In the second step, these 514 compounds were docked into the active site of the biotin binding site of the biotin-pseudoknot using FlexX, and ranked by FlexX scoring function.³⁰ The active site was defined as all residues within 6.5 Å of the reference ligand, biotin, in the biotin-pseudoknot. The active site included 9 residues (G6, U7, A16, C17, G18, A24, A25, A26, G27, and Mg 6). The nucleic acid residues, U7 and A26, are key residues that interact with biotin.²⁶ Eighty-six compounds that were highly-ranked in the FlexX output as occupying the biotin-binding pocket were selected for a final intensive docking analysis. The final docking analysis was performed using FlexX combined with the consensus scoring function, CScore.³⁰ In our score analysis, any docked pose of the structures with a CScore greater than 4 was visually inspected for further consideration, because several conformers had bad position in the active site. Optimal score was calculated as the ratio of the number of conformers bound properly in the active site to the total number of conformers with CScores above 4. Among the 86 candidates, compounds with a CScore below 3 were consistently considered poor and so were dropped from consideration. After final filtering with FlexX, together with the CScore values, 58 compounds were selected to examine their effect on –1 frameshifting efficiency in biological assays.

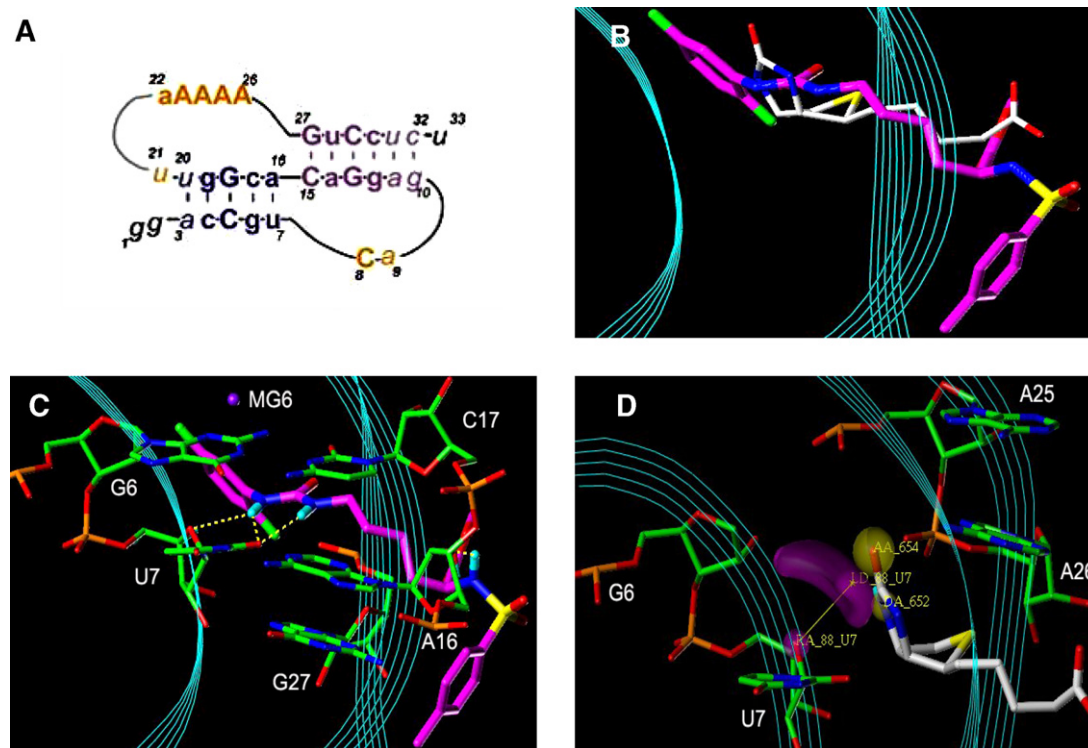


Figure 1. (A) The biotin-pseudoknot RNA sequence used for this study.²⁶ (B) Overlay of FlexX-docked pose of h4 and X-ray pose of biotin in the biotin-pseudoknot. The ligand is rendered in capped stick. Carbon atoms of h4 are magenta and those of biotin are white. Oxygen atoms of the ligands are red; nitrogen blue; fluorine green; and sulfur yellow. Hydrogen atoms are omitted for clarity. Cyan lined-ribbon represents the back bone of biotin-pseudoknot. (C) Docked model of h4 in complex with biotin-pseudoknot complex. The residues in the active site of biotin-pseudoknot are rendered in stick. Carbon atoms of pseudoknot are green; oxygen red; nitrogen blue; and phosphorus orange. Yellow dashed lines are hydrogen bond and the distance is less than 2.5Å. (D) X-ray pose²⁶ of biotin in the active site and the pharmacophore queries for the Unity search. The hydrogen bonding acceptor is shown as yellow sphere and acceptor site is shown as magenta sphere and ribbon.

2.2. In vitro transcription/translation (TNT[®])-coupled assay

We hypothesized that selected candidate compounds would bind to the biotin-pseudoknot and affect -1 RF that is regulated by the biotin-pseudoknot. To examine the effect of these 58 compounds on -1 RF, in vitro transcription/translation (TNT[®])-coupled assays were conducted in rabbit reticulocytes using the template construct shown in Figure 2A. If a -1 RF occurs at the slippery sequence, the termination codon of the *Renilla* luciferase gene (*rluc*) is not read and translation proceeds through the firefly luciferase gene (*fluc*), resulting in the production of an *rluc*–*fluc* fusion protein. The -1 frameshifting efficiencies in the presence of selected compounds were measured both by sodium dodecyl sulfate polyacrylamide gel electrophoresis (SDS–PAGE) and dual luciferase assays. First, we determined -1 frameshifting efficiencies by SDS–PAGE; the results are shown in Figure 2B. The *rluc*–*fluc* fusion product yields a 100-kDa protein containing 22 methionine residues, whereas the non-frameshifting *rluc* protein product is 40 kDa with 9 methionines. Therefore, frameshifting efficiencies (%) were calculated using the formula $(I[RF]/22)/[(I[RF]/22)+(I[NRF]/9)]$, where $I[RF]$ is the signal intensity of the frameshifting product (RF) and $I[NRF]$ is the signal intensity of the non-frameshifting product. Dimethyl

sulfoxide (DMSO) was considered as a control because all test compounds were dissolved in DMSO. The frameshifting (100 kDa) and non-frameshifting (40 kDa) proteins are marked with arrows in Figure 2B. The fold change in -1 RF was determined by calculating the ratio of -1 frameshifting efficiency in the presence of compounds versus that in the absence of compounds. Six compounds (e7, h5, b5, e4, h4, and h2) shown in Figure 3A, increased -1 RF, and h4 noticeably increased -1 frameshifting efficiency up to 13.67% (Fig. 2B, lane 7), approximately 19-fold greater than the 0.71% efficiency observed in control (Fig. 2B, lane 1). Other compounds (e7, h5, b5, e4, and h2) afforded 2- to 15-fold increase in -1 frameshifting efficiency.

To encapsulate the SAR (structure–activity relationships) features of the hit compounds, we built a pharmacophore by using the GALHAD³² program. As shown in Figure 3B, all six hit molecules and biotin are superimposed nicely onto the pharmacophore model, implying that they may bind to biotin-pseudoknot in a similar mode. The key pharmacophoric elements include two hydrophobic features derived from six hit compounds that increase the -1 frameshifting. Two hydrogen bond acceptors and one donor features are common to all the molecules aligned including the template biotin. The results suggest that additional hydrophobic

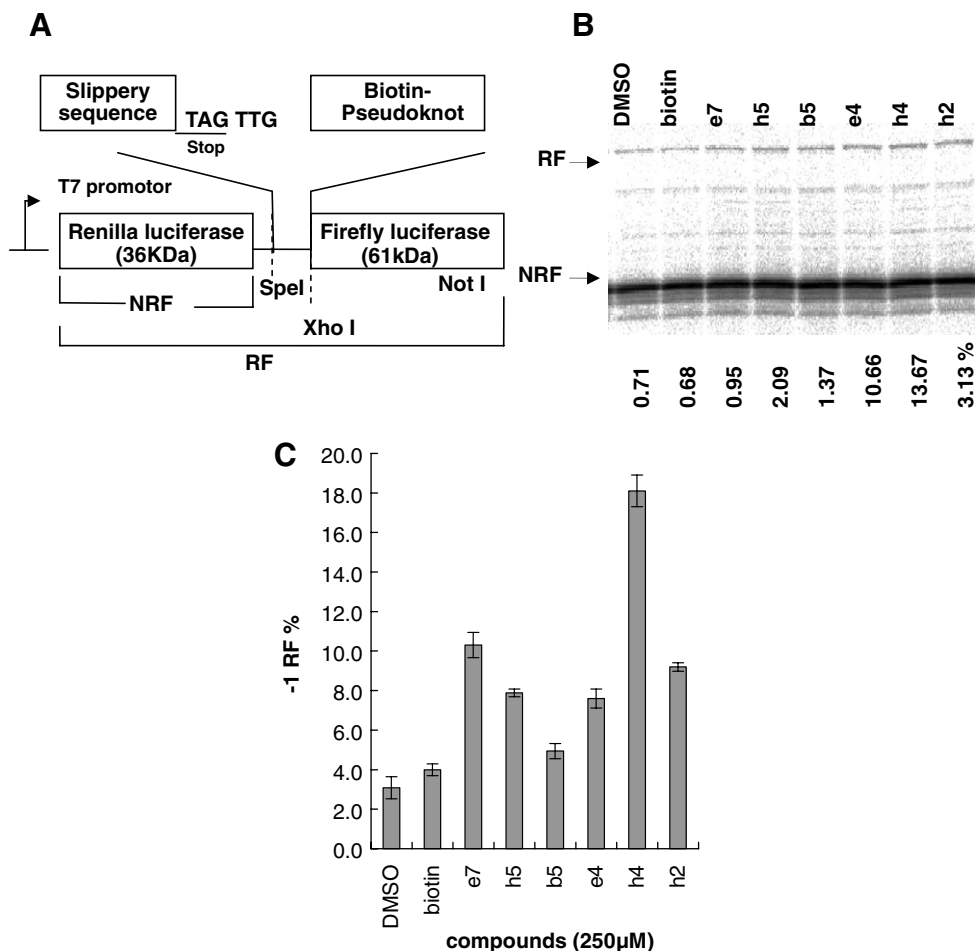


Figure 2. (A) Template construct for -1 frameshifting assay. (B and C) -1 frameshifting efficiencies induced by biotin-pseudoknot in the presence of compounds ($250 \mu\text{M}$) determined by SDS-PAGE (B) and dual luciferase assay (C). The $-1\text{RF} \%$ values are shown at the bottom of autoradiogram of SDS-PAGE. Each $-1\text{RF} \%$ value from dual luciferase assay is the average of triplicate experiments.

moieties in hit compounds may contribute to stabilize the biotin-pseudoknot structure and increase the -1 frameshifting efficiency.

To confirm the -1 frameshifting efficiency values determined by SDS-PAGE, we also measured the efficiencies by dual luciferase assay,³³ which quantifies the amount of reporter proteins produced and gives more accurate -1 frameshifting efficiency values. The results of the dual luciferase assay are shown in Figure 2C. The -1 frameshifting efficiency with DMSO is 3.0%. Compound h4 promoted -1 frameshifting efficiency by 18.1%, 6-fold greater than the control. Other compounds also promoted -1 frameshifting efficiency. The fold changes in -1 frameshifting efficiency calculated by the two assay methods are quite different. However, both assays commonly reveal that only six compounds (e7, h5, b5, e4, h4, and h2) out of the 56 tested compounds increased -1RF induced by biotin-pseudoknot and that h4 produced the highest increase. Concentration dependence of the activity of h4 was examined by *in vitro* TNT assay. The results of assay in the presence of the indicated concentrations (25 nM to $250 \mu\text{M}$) of h4 were shown in Figure 4A. The results revealed that h4 increased the -1RF in a concentration-dependent manner, and interestingly, it increased the -1RF efficiency even at nano-

molar concentration in comparison with that in the presence of biotin (the control) at $250 \mu\text{M}$.

2.3. Cell-based -1 frameshifting assay

A cell-based TNT-coupled assay was performed to confirm the *in vitro* assay results. For this experiment, human embryonic kidney cells (HEK 293) were transfected with a construct containing the template shown in Figure 2A. -1 frameshifting efficiencies were measured by conducting dual luciferase assays on the cell extract, and the results are shown in Figure 4B. Basal level of -1 frameshifting efficiency is 3.0% (DMSO only), while the efficiency is 8.05% in the presence of h4. As in the *in vitro* TNT assays, compound h4 significantly increased the -1RF in the cell.

2.4. Selectivity of h4 for biotin-pseudoknot

The candidate compounds were selected by virtual screening to target biotin-pseudoknot RNA, and compound h4 had a significant effect on the -1RF induced by biotin-pseudoknot. To investigate whether h4 interacts with our target and affects the -1RF , we compared the effect of h4 on the -1RF system induced by the RNA pseudoknot of Pea Enation Mosaic Virus (PEMV)

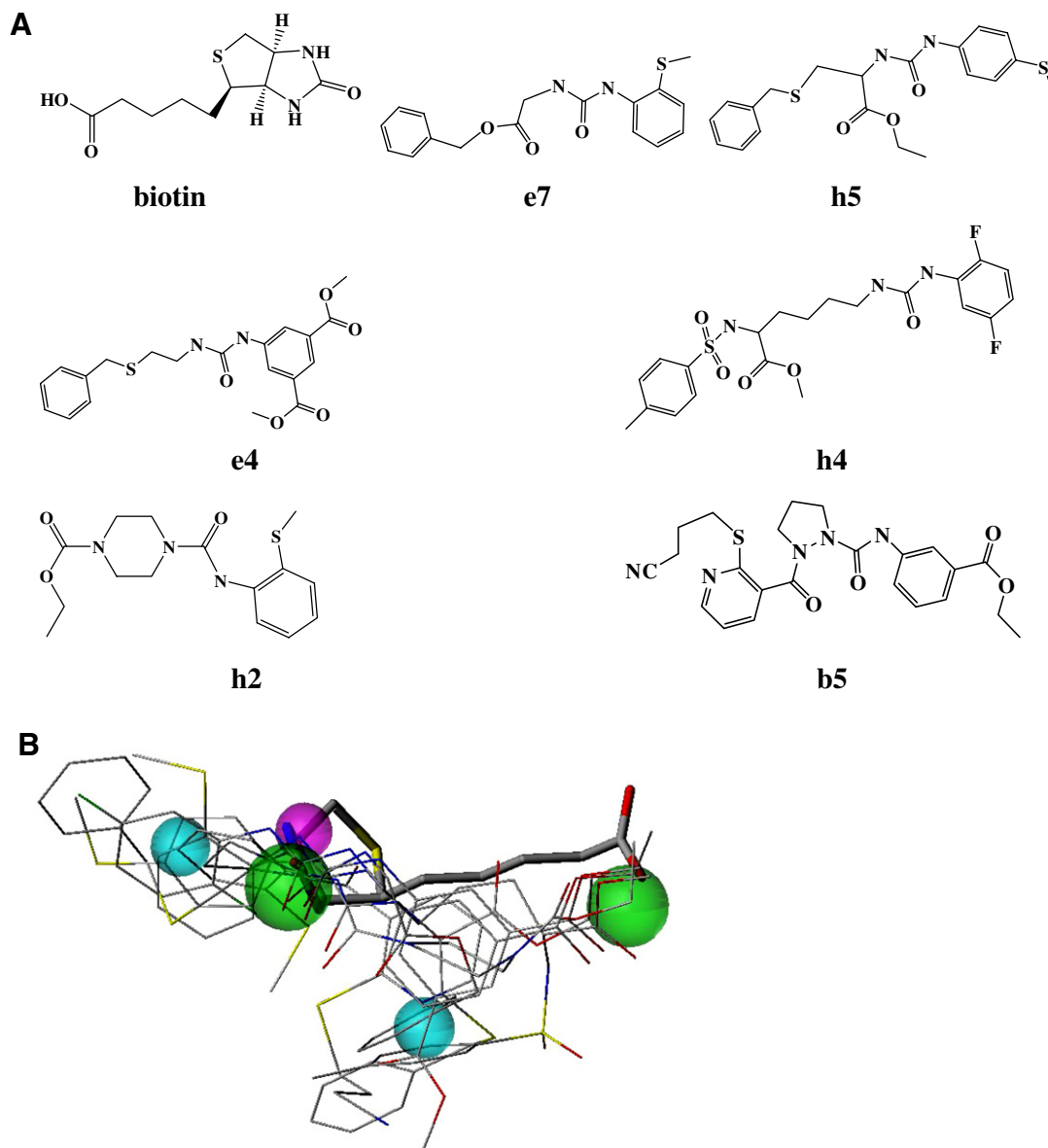


Figure 3. (A) Structures of biotin and the hit compounds that increases the -1 RF efficiency in the in vitro -1 frameshifting assay. (B) The GALAHAD³² pharmacophore model derived from all six hit molecules and biotin. Pharmacophore features are displayed by spheres: two hydrophobic centers (cyan), two H-bond acceptor atoms (green), and one H-bond donor atom (magenta). The template biotin is rendered as capped stick.

pseudoknot). PEMV-pseudoknot has sequence and structure, completely different from those of biotin-pseudoknot.^{25,34} Using a template construct that contains the PEMV-pseudoknot instead of the biotin-pseudoknot, we measured the -1 frameshifting efficiency by in vitro TNT-coupled assays. Translation products were measured by SDS-PAGE and dual luciferase assays. The results from the SDS-PAGE are illustrated in Figure 5A. The -1 frameshifting efficiency in the presence of h4 (7.60%) is similar to that of control (6.87%), and biotin slightly decreased the -1 RF. The results from dual luciferase assays are also shown in Figure 5B. Similar to the SDS-PAGE results, h4 does not alter the -1 RF induced by the PEMV-pseudoknot. These results strongly suggest that h4 should interact selectively with the biotin-pseudoknot and increase the

-1 RF. In addition, we inspected whether h4 affected only the translation step by interacting with the RNA structure. In the presence of h4, in vitro transcription and in vitro translation assays were conducted separately (see the Supplementary Figure S1), and we confirmed that h4 interrupts the translation step, but not transcription.

2.5. Docked model of h4 in complex with biotin-pseudoknot

The FlexX-docked mode of h4, which shows the highest enhancement of -1 frameshifting efficiency, is shown in Figure 1C. The hit compound h4 (-23.4 kcal/mol) was ranked higher than biotin (-19.1 kcal/mol) in the FlexX binding energy score output. Compound h4 is bound at

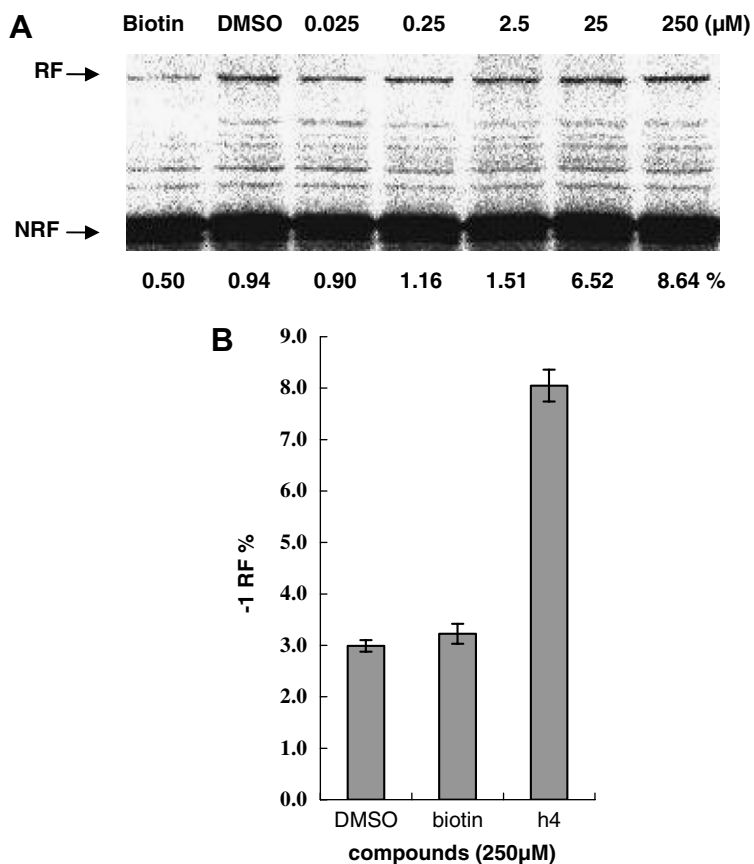


Figure 4. In vitro and cell-based -1 frameshifting assays in the presence of h4. (A) Concentration-dependent effect of the best hit compound (h4) on the -1 RF determined by in vitro TNT coupled assay and SDS-PAGE. The -1 RF % values are shown at the bottom of autoradiogram. The concentration of biotin used in this experiment is 250 μM . (B) Comparison of -1 frameshifting efficiency in the presence of biotin versus h4 by cell-based experiment.

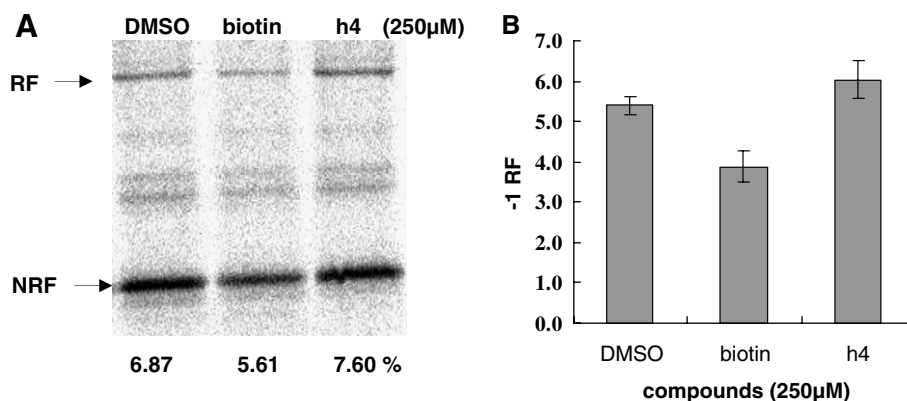


Figure 5. In vitro -1 frameshifting assay using the -1 RF system containing PEMV-pseudoknot. -1 Frameshifting efficiencies induced by PEMV-pseudoknot in the presence of biotin and h4 determined by SDS-PAGE (A) and dual luciferase assay (B). Each -1 RF % value from dual luciferase assay is the average of triplicate experiments.

the interface between the two stems (stem1 and stem2) and interacts with the last nucleotide of stem 1 (U7) by forming multiple hydrogen bonds. This docking mode is similar to the binding pose of biotin in the X-ray structure (Fig. 1B). As shown in Figure 1C, the difluoro-phenyl ureidyl group of h4 fits into the binding pocket for the ureido ring of biotin. Ureidyl NH groups of h4 form hydrogen bonds with O4' and 2-carbonyl oxygen of uracil ring of U7, respectively, and NH of

the sulfonamido group forms a hydrogen bond with ribose O2' atom of A16 in stem 1. Compound h4 interacts with U7, one of the critical residues for interaction with biotin in the X-ray structure. In addition, h4 interacts with more residues in the RNA pseudoknot than biotin does, which may increase the stability of the biotin-pseudoknot. As a result, the pseudoknot complexed with h4 may increase the time that the ribosome pauses on the slippery site, resulting in an increase of -1 RF. In

studies of peptidyl transferase inhibitors, longer stalled time of the ribosome on the slippery site strongly increased the -1 frameshifting efficiencies.³⁵

3. Conclusion

The aim of this study was to identify small molecule ligands that can selectively interact with the biotin-pseudoknot through virtual screening of a chemical database. We performed a computational screening against the biotin-pseudoknot using FlexX and CScore program. After virtual screening, -1 RF in the presence of select compounds was measured by in vitro and cell-based -1 frameshifting assays.

Through this study, we first discovered novel compounds that interact with the biotin-pseudoknot to alter the -1 frameshifting efficiencies. Our approach can be applied for the discovery of small molecules that interact with specific viral RNA structures that induce -1 RF in many pathogenic viruses, such as SARS coronavirus and HIV-1.

4. Experimental

4.1. Determination of pharmacophores based on the X-ray structure of biotin-binding pseudoknot

Unity Search and docking studies were performed with Tripos Sybyl program³⁰ on SGI Octan II (R12000, 400 MHz MPS process) workstation with the IRIX 6.5 operating system. We used the crystal structure of the biotin-pseudoknot (PDB id: 1F27) obtained from Protein Data Bank. We extracted biotin from 1F27 to use as the reference ligand. A commercially-available chemical database³¹ was used in Unity 2D and 3D search for structures that interact similarly to biotin. The pharmacophore query for Unity search consisted of a hydrogen bond acceptor atom and a hydrogen bond acceptor site. The acceptor atom is the ureido carbonyl oxygen atom of biotin, which forms a hydrogen bond with exocyclic 2NH_2 of G6. The acceptor site is the ribose O4' atom of U7 residue, one of the key residues in the biotin-binding pocket. All selected compounds were energy-minimized with the standard Tripos force field, after Gasteiger–Hückel charges were assigned for the ligand atoms. The minimization was run until the energy converged to a maximum derivative of $0.001 \text{ kcal mol}^{-1} \cdot \text{Å}^{-1}$.

4.2. FlexX/CScore filtering

The docking and subsequent scoring were performed using the default parameters of the FlexX program combined with the consensus scoring function (CScore) implemented in Sybyl. The active site region was defined as a sphere within 6.5 Å of the reference ligand (biotin). All residues in the active site were assigned as templates. The main setting was set with 1000 solutions in order to find the maximum conformers for each compound. The CScore module consists of five scoring functions: GOLD-like function (G-score), DOCK-like function

(D-score), Chemscore, PMF, and FlexX score (F-score). Each scoring function casts a vote of 1 for a compound that is in the best half or 0 otherwise. By adding all votes, CScore gives a consensus score that ranges from 0 to 5.

4.3. Pharmacophore modeling

Pharmacophore alignment of multiple ligands was generated and analyzed with the GALAHAD³² program, integrated in Tripos Sybyl 7.3 software package based on Red-Hat Linux 3.0.5.

Seven compounds (e7, h5, e4, h4, h2, b5, and biotin) were used to build the pharmacophore. The structure of biotin extracted from the X-ray structure of the biotin-binding pseudoknot (PDB id: 1F27) was used as a template for the alignment. GALAHAD's default parameters cover six feature types: hydrogen bond donor and acceptor atoms; positive nitrogen; negative and hydrophobic centers; and steric features, and generate 20 pharmacophoric hypotheses. The best optimal model was selected out of these 20 models based on the most reasonable pharmacophoric overlap and steric consensus (Fig. 3B).

4.4. Template constructs for -1 frameshifting assay

When annealed, appropriate ends of the template construct were ligated into XhoI/ SpeI restriction sites of the dual luciferase vector. The biotin-binding RNA pseudoknot sequence (5'-GGACCGUCAGAGGACACGGUUA AAAAGUCCUCU-3') was inserted into p2luc. We also made construct including PEMV-pseudoknot sequence (5'-GAAUCCGGUCGACUCCGGAGAAACAAAGUCA-3') to identify selectivity of candidate compounds for biotin-pseudoknot. Alternatively, DNA templates containing a T7 promoter were transcribed and translated using the in vitro TNT T7-transcription/translation-coupled reticulocyte lysate. The UAG termination codon of the *Renilla* luciferase gene (rluc), purified from *Renilla reniformis*, is located immediately after the slippery sequence. The pseudoknot RNA is located 6 residues downstream. If an -1 RF occurs at the slippery sequence, the termination codon of the *Renilla* luciferase gene is not read, and translation proceeds through the firefly luciferase gene (fluc) purified from *Photinus pyralis*, resulting in the production of an rluc-fluc fusion protein (Fig. 2A).

4.5. In vitro transcription/translation-coupled (TNT[®]) assay

All plasmids were isolated by alkaline lysis and further purified by phenol/chloroform extraction and ethanol precipitation. The lyophilized DNA was dissolved in water. The TNT T7-coupled transcription/translation system (Promega) was used according to the manufacturer's protocol. Template plasmid (500 ng) was used in a $20 \mu\text{l}$ reaction containing $16 \mu\text{l}$ of reticulocyte lysate, $0.8 \mu\text{l}$ of $10 \mu\text{Ci}/\mu\text{l}$ [³⁵S]-labeled methionine (NEN), and $0.5 \mu\text{l}$ of 100 mM candidate compounds. To separate the rluc-fluc fusion protein from the rluc protein, the samples were run on 12% sodium dodecyl sulfate polyacrylamide gels (SDS-PAGE). After electrophoresis,

the gels were dried and exposed to PhosphorImager screens; the signals were then quantified. The product identity was confirmed by SDS–PAGE and dual luciferase analysis.

4.6. Dual luciferase assay

Promega's Dual-Luciferase[®] Reporter (DLR[™]) assay system provides an efficient means of performing dual luciferase assays. The activities of firefly and *Renilla* luciferases are measured sequentially from a single sample. The translation products are transferred into the luminometer tube containing 50 μ l of luciferase assay reagent II (Promega) and mixed by brief vortexing; the tube is then placed in the TD-20/20 luminometer (Turner Designs) and firefly luciferase activity is measured. After quantifying the firefly luminescence, this reaction is quenched, and the *Renilla* luciferase reaction is initiated by simultaneously adding 50 μ l of Stop and Glo[®] Reagent to the same tube. Light emission is recorded for 10 s, respectively, for both luciferases and the ratio of the two measurements is calculated. The NRF product is the *Renilla* luciferase protein, and the RF product is the firefly luciferase protein. Frameshifting efficiencies were calculated by the formula $\% = [(\text{firefly luciferase of sample} / \text{Renilla luciferase of sample}) / (\text{firefly luciferase of p2luci} / \text{Renilla luciferase of p2luci})] \times 100$. Plasmid p2luci, which expresses an in-frame *Renilla*–firefly fusion protein, was used as a positive control for –1RF (defined as 100% efficiency). All individual in vitro assays to determine the average frameshifting efficiencies were repeated three times.

4.7. Cell-based –1 frameshifting assay

The human embryonic kidney cell line, HEK 293, was cultured in Dulbecco's modified Eagle's medium (DMEM) (Sigma) containing 1% penicillin–streptomycin (Hyclone) and supplemented with 10% fetal bovine serum (Hyclone). For cell-based dual-luciferase assays, cells were subcultured to 40% confluence in 24-well plates. Cells were transfected using JetPEI (Qbiogen). Mixture of DNA (50 ng) and 2 μ l of JetPEI (Qbiogen) were transfected and incubated for 18 h. Next, 2 μ l of candidate compounds dissolved in DMSO was added and incubated for another 18 h. The cells were assayed for transient expression of reporter genes 36 h after the transfection. For dual luciferase assays, cells were washed twice with PBS, and 150 μ l of passive lysis buffer (Promega) was dispensed to each culture well. The cells were then lysed by rocking the culture plates at room temperature for 30 min and spun to pellet cell debris. The concentration of protein was measured by Bradford assay and 50 μ g of each sample was prepared. 1 μ l of supernatant was taken, and luciferase activities were determined using the Dual Luciferase[™] Reporter Assay System (Promega) as previously described.

Acknowledgments

This work was supported by the Basic Research Program of the Korea Science and Engineering Foundation

(Grant No. R04-2003-000-10099-0), and in part by the Korea Research Foundation Grant (KRF-2002-015-CS0027).

Supplementary data

Supplementary data associated with this article can be found, in the online version, at [doi:10.1016/j.bmc.2008.02.025](https://doi.org/10.1016/j.bmc.2008.02.025).

References and notes

- Brierley, I. J. *Gen. Virol.* **1995**, *76*, 1885.
- Jacks, T.; Varmus, H. E. *Science* **1985**, *230*, 1237.
- Chamorro, M.; Parkin, N.; Varmus, H. E. *Proc. Natl. Acad. Sci. U.S.A.* **1992**, *89*, 713.
- ten Dam, E.; Brierley, I.; Inglis, S.; Pleij, C. *Nucleic Acids Res.* **1994**, *22*, 2304.
- Brierley, I.; Rolley, N. J.; Jenner, A. J.; Inglis, S. C. *J. Mol. Biol.* **1991**, *220*, 889.
- Tzeng, T. H.; Tu, C. L.; Bruenn, J. A. *J. Virol.* **1992**, *66*, 999.
- Kang, H.; Tinoco, I., Jr. *Nucleic Acids Res.* **1997**, *25*, 1943.
- Jacobs, J. L.; Belew, A. T.; Rakauskaitė, R.; Dinman, J. D. *Nucleic Acids Res.* **2007**, *35*, 165.
- Peltz, S. W.; Hammell, A. B.; Cui, Y.; Yasenchak, J.; Puljanowski, L.; Dinman, J. D. *Mol. Cell. Biol.* **1999**, *19*, 384.
- Shehu-Xhilaga, M.; Crowe, S. M.; Mak, J. J. *J. Virol.* **2001**, *75*, 1834.
- Goss Kinzy, T.; Harger, J. W.; Carr-Schmid, A.; Kwon, J.; Shastry, M.; Justice, M.; Dinman, J. D. *Virology* **2002**, *300*, 60.
- Brierley, I.; Jenner, A. J.; Inglis, S. C. *J. Mol. Biol.* **1992**, *227*, 463.
- Dinman, J. D.; Wickner, R. B. *J. Virol.* **1992**, *66*, 3669.
- Gesteland, R. F.; Atkins, J. F. *Annu. Rev. Biochem.* **1996**, *65*, 741.
- Naphine, S.; Liphardt, J.; Bloys, A.; Routledge, S.; Brierley, I. *J. Mol. Biol.* **1999**, *288*, 305.
- Bertrand, C.; Prère, M. F.; Gesteland, R. F.; Atkins, J. F.; Fayet, O. *RNA* **2002**, *8*, 16.
- Paul, C. P.; Barry, J. K.; Dinesh-Kumar, S. P.; Brault, V.; Miller, W. A. *J. Mol. Biol.* **2001**, *310*, 987.
- Giedroc, D. P.; Theimer, C. A.; Nixon, P. L. *J. Mol. Biol.* **2000**, *298*, 167.
- Yusupova, G. Z.; Yusupov, M. M.; Cate, J. H.; Noller, H. F. *Cell* **2001**, *106*, 233.
- Dinman, J. D.; Richter, S.; Plant, E. P.; Taylor, R. C.; Hammell, A. B.; Rana, T. M. *Proc. Natl. Acad. Sci. U.S.A.* **2002**, *99*, 5331.
- Plant, E. P.; Jacobs, K. L. M.; Harger, J. W.; Meskauskas, A.; Jacobs, J. L.; Baxter, J. L.; Petrov, A. N.; Dinman, J. D. *RNA* **2003**, *9*, 168.
- Namy, O.; Moran, S. J.; Stuart, D. I.; Gilbert, R. J.; Brierley, I. *Nature* **2006**, *441*, 244.
- Kolk, M. H.; van der Graaf, M.; Wijmenga, S. S.; Pleij, C. W.; Heus, H. A.; Hilbers, C. W. *Science* **1998**, *280*, 434.
- Dinman, J. D.; Ruiz-Echevarria, M. J.; Peltz, S. W. *Trends Biotechnol.* **1998**, *16*, 190.
- Nixon, P. L.; Rangan, A.; Kim, Y. G.; Rich, A.; Hoffman, D. W.; Hennig, M.; Giedroc, D. P. *J. Mol. Biol.* **2002**, *322*, 621.
- Nix, J.; Sussman, D.; Wilson, C. *J. Mol. Biol.* **2000**, *296*, 1235.
- Marciniak, R. A.; Sharp, P. A. *EMBO J.* **1991**, *10*, 4189.

28. Lind, K. E.; Du, Z.; Fujinaga, K.; Peterlin, B. M.; James, T. L. *Chem. Biol.* **2002**, *9*, 185.
29. Filikov, A. V.; Mohan, V.; Vickers, T. A.; Cook PD, R. H.; Abagyan, R. A. *J. Comput. Aided Mol. Des.* **2000**, *14*, 593.
30. Sybyl, 6.9 ed.; SYBYL molecular modeling software, Tripos Inc., St. Louis, MO, 2003.
31. LeadQuest Chemical Compounds Libraries (Version February **2004**), Tripos Discovery Research Ltd., UK, 2004.
32. Richmond, N. J.; Abrams, C. A.; Wolohan, P. R.; Abrahamian, E.; Willett, P.; Clark, R. D. *J. Comput. Aided Mol. Des.* **2006**, *20*, 567.
33. Grentzmann, G.; Ingram, J. A.; Kelly, P. J.; Gesteland, R. F.; Atkins, J. F. *RNA* **1998**, *4*, 479.
34. Egli, M.; Minasov, G.; Su, L.; Rich, A. *Proc. Natl. Acad. Sci. U.S.A.* **2002**, *99*, 4302.
35. ten Dam, E.; Pleij, K.; Draper, D. *Biochemistry* **1992**, *31*, 11665.